Aircraft Electric Anti-skid Braking System Based on Fuzzy-PID Controller with Parameter Self-adjustment Feature

Wei Xiaohui(魏小辉)*, *Yin Qiaozhi*(尹乔之), *Nie Hong*(聂宏)
Zhang Ming(张明), *Tao Zhouliang*(陶周亮)

State Key Laboratory of Mechanics and Control of Mechanical Structure, Nanjing University of Aeronautics and Astronautics, Nanjing, 210016, P. R. China

(Received 13 June 2013; revised 09 December 2013; accepted 15 December 2013)

Abstract: The principle of electric braking system is analyzed and an anti-skid braking system based on the slip rate control is proposed. The fuzzy-PID controller with parameter self-adjustment feature is designed for the anti-skid braking system. The dynamic model of aircraft ground braking is established in the simulation environment of MATLAB/SIMULINK, and simulation results of dry runway and wet runway are presented. The results show that the fuzzy-PID controller with parameter self-adjustment feature for the electric anti-skid braking system keeps working in the state of stability and the brake efficiencies are increased to 93% on dry runway and 82% on wet runway respectively.

Key words: electric braking system; slip rate; anti-skid braking; fuzzy-PID controller
CLC number: V226 **Document code**: A **Article ID**: 1005-1120(2014)01-0111-08

1 Introduction

Electric braking system is an irresistible development trend of the aircraft braking system at present. Because of its complicated non-linear behavior, the selection of control law is of great importance, which has a bearing on the performance of the whole system. So according to the features of the electric braking system, it is necessary to improve the anti-skid control method of the braking system to achieve the best possible braking efficiency.

Nowadays, most of the anti-skid control systems which have been put into use in domestic apply the sliding velocity control system[1] (using pressure-bias-modulated (PBM)), while several commercial and military jet aircrafts in Europe use slip rate control braking system[2]. In comparison, the efficiency of the sliding velocity control system is higher[3-6]. As the theory of control developing, intelligent control has been more and more widely applied into practical engineering, which brings a new idea to design the control law of aircraft braking system. Some new control theory, like fuzzy control[7], neural network control[8], optimum control[9], and nonlinear control[10] has all been used to design the anti-skid law.

According to the algorithm of fuzzy-proportional-integral-derivative (PID) control with parameter self-adjustment feature, the anti-skid law of the electric braking system is designed in this paper. At the same time, the braking performance is simulated in the cases of dry runway and wet runway to verify the advantages of the electric braking system, as well as the high efficiency of the control law.

2 Electric Braking System Based on Slip Rate Control

The definition of the slip rate is the relative slippage between the wheel and the road. Its ex-

Foundation items: Supported by the National Natural Science Foundation of China (51105197, 51305198, 11372129); the Project Funded by the Priority Academic Program Department of Jiangsu Higher Education Instructions.

* **Corresponding author**: Wei Xiaohai, Associate Professor, E-mail: wei_xiaohui@nuaa.edu.cn.

pression can be shown as follows

$$\sigma = \frac{v_x - v_r}{v_x} \tag{1}$$

where σ is the slip rate, v_x the heading landing speed of the aircraft, and v_r the linear velocity of the wheel.

The slip rate has the greatest influence on the friction coefficient. Therefore, the braking system should control the slip rate on the optimal value in order to keep the friction coefficient maximal and to achieve the highest efficiency of braking.

The aircraft electric braking system contains five parts below: Electromechanically actuated (EMA) braking frame, wheel speed sensor and its bracket, torque transducer and its bracket, EMA controller, and B/S controller. The operating principle is: The signal of wheel speed and brake torque is transmitted to B/S controller through the wheel speed sensor and the torque transducer. The signal generated by B/S controller is then imported to EMA controller, which will produce control signal to control EMA mechanism. This EMA mechanism exports brake pressure on brake disc to generate the corresponding brake torque. As a result, electric braking system is the double-negative-feedback closed-loop control system based on the wheel speed and the brake torque. Fig. 1 shows its working principle.

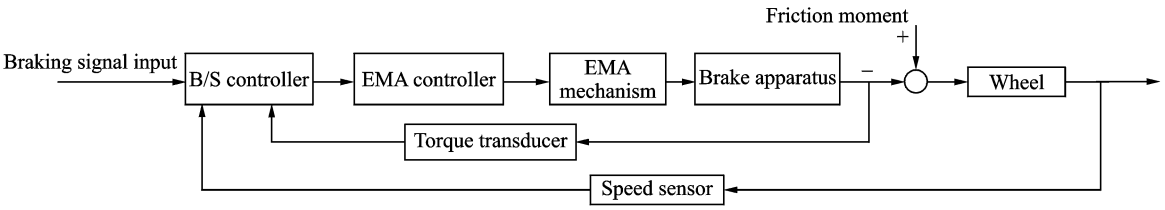

Fig. 1 Schematic diagram of electric braking system

3 Fuzzy-PID Controller with Parameter Self-adjustment Feature

3.1 Basic ideas of fuzzy-PID control algorithm

The fuzzy-PID control system with parameter self-adjustment feature[11] is an adaptive control system which uses the fuzzy control rule to modify the PID parameters online. It is able to realize better dynamic and steady-state performance for nonlinear time-varying system.

The control signal of the conventional digital PID adjuster is

$$U(k) = K_P E(k) + K_I \sum E(k) + K_D(E(k) - E(k-1)) \tag{2}$$

where $U(k)$ is the output of PID controller, K_p the proportionality coefficient of the PID controller, K_I the integral coefficient, K_D the differential coefficient, $E(k)$ the closed-loop deviation, and $E(k-1)$ the closed-loop deviation at the last time.

The fuzzy-PID controller applies the fuzzy set theory to establish the functions of K_P, K_I, K_D, deviation absolute value $|E|$, and deviation change $|EC|$ based on the regular PID controller, shown as

$$\begin{aligned} K_P &= f_1(|E|, |EC|) \\ K_I &= f_2(|E|, |EC|) \\ K_D &= f_3(|E|, |EC|) \end{aligned} \tag{3}$$

K_P, K_I, K_D can be adjusted online according to different $|E|$ and $|EC|$.

3.2 Modeling of fuzzy-PID controller with parameter self-adjustment feature

The model of the fuzzy-PID controller with parameter self-adjustment feature is established with MATLAB/SIMULINK. From the above analysis, the electric braking system contains not only the velocity feedback, but also the feedback of brake torque, of which the brake torque is on the inner loop, and the slip rate is on the outer loop. The control block diagram of the whole braking system is shown in Fig. 2.

Due to the double-close-loop control, the control parts consist of the slip rate and the brake torque. The design of the fuzzy-PID control above mainly targets the control of the slip rate. However, the control of the brake torque uses traditional PID control method, aiming to generate the

signal to adjust the rotating speed of DC motor according to the difference of the brake torque between the input and the actual values, which can make the actual brake torque track the target value. Thus the model of the braking controller of the electric braking system is established.

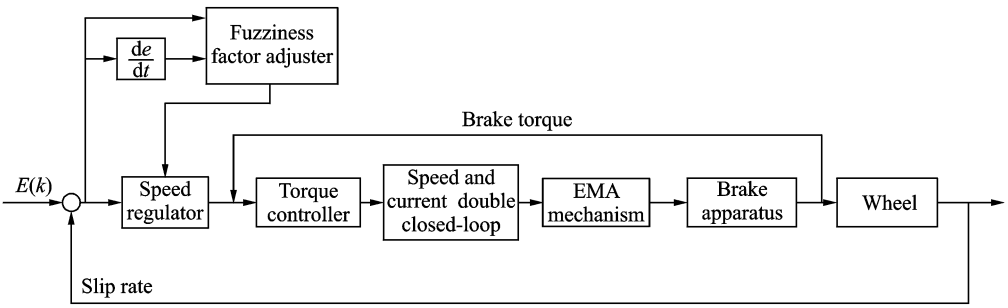

Fig. 2 Control block diagram of electric braking system

4 Aircraft Ground Taxiing Model

When the aircraft is taxiing on the ground, the forces on the aircraft are: Gravity, motor power, aerodynamic force (including lift, drag), ground reaction force and friction force[12] on the wheels, and the moment produced by the forces. The force analysis of airplane movement on the ground is shown in Fig. 3.

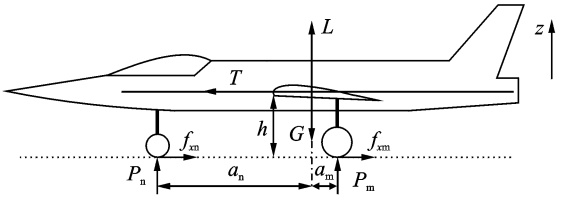

Fig. 3 Force analysis of airplane movement on ground

The external resultant force and the moment in the ground axis system are

$$\begin{cases} T-D-Q_n-2Q_m=m\ddot{x} \\ P_n+2P_m+L-G=m\ddot{z} \\ P_n \cdot a_n\cos\theta-P_m \cdot a_m\cos\theta-M_T-(Q_n+2Q_m)y=I_b\ddot{\theta} \end{cases} \tag{4}$$

where T is the motor power. D and L are the air drag and the lift respectively, Q_n, Q_m the friction forces to the nose wheel and one of the main wheel respectively, P_n, P_m the ground reaction forces to the nose wheel and one of the main wheel. G is the gravity, a_n the projection distance between the nose wheel and the gravity center of the aircraft, a_m the projection distance between the main wheels and the gravity center of the aircraft, m the weight of the aircraft, M_T the moment of the motor, I_b the moment of inertia of the aircraft, and θ the pitch angle.

5 Model of Electric Differential Braking System

5.1 Model of EMA mechanism

The EMA mechanism is composed of brushless DC motor, harmonic reducer and ball screw[13]. The inertia moment, the driving moment and the drag torque of the ball screw are the important bases in selecting the motor capacity when the system is designed.

The load torque of the motor is

$$T_M=J_M\dot{\omega}_h+T_L \tag{5}$$

where T_M is the load torque of the motor, $\dot{\omega}_h$ the angular acceleration of the ball screw, J_M the rotational inertia, and T_L the part of load torque of the motor caused by ball screw and drag torque.

The motor drives the ball screw to change rotational motion to rectilinear motion of the nut, which will push the pressure plate against the brake disc. So the formula is

$$\frac{\omega_h t}{2\pi}=\frac{l}{L_0} \tag{6}$$

where ω_h is the rotational speed of the ball screw, l the axial displacement of the datum point of the nut.

The revolving speed and current feedback direct current governor system is composed of DC motor and motor controller, which has nice static and dynamic performance[11]. The revolving speed and current close-loops are both adjusted by PI controller. The voltage and current of the circuit are shown as

$$u_a(t)-E_a=R_a\left(T_l\frac{di_a(t)}{dt}+i_a(t)\right) \tag{7}$$

$$i_a(t)-i_{al}(t)=\frac{T_m dE_a(t)}{R_a dt} \tag{8}$$

where T_l is the electromagnetic time constant of armature loop, R_a the armature resistance, E_a the counter electromotive force of the motor, $i_{al}(t)$ the load current, and T_m the electromechanical time constant.

According to the transfer function of PWM power electronic converter and the calculation of the feedback factors, the mathematical model of the direct current governor system[14] is shown in Fig. 4.

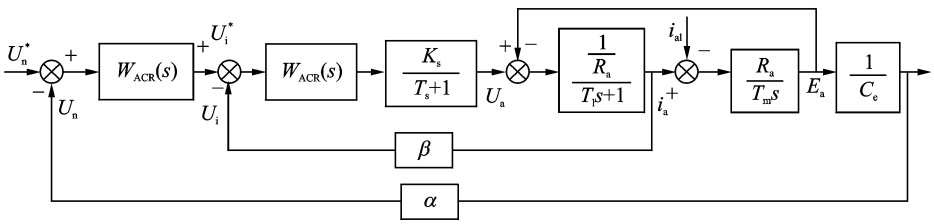

Fig. 4 Mathematical model of direct current governor system

5.2 Model of brake apparatus

The main effect of the brake apparatus is to change braking thrust into braking torque as well as to consume the kinetic energy of the aircraft.

The braking thrust S_t is in proportion to the compact distance l approximately, which is shown as follow

$$S_t = K_t l \tag{9}$$

where K_t is the proportionality coefficient.

The braking torque can be derived according to the braking force, shown as

$$M_b = \mu_{mc} \cdot N_{mc} S_t \cdot (R_t + r_t)/2 \tag{10}$$

where μ_{mc} is the friction coefficient, N_{mc} the numbers of the friction faces, R_t the external radius of the stators, and r_t the internal radius of the rotors.

However, the brake pair not only usually suffers deformation during mechanical wear and temperature variation, but is also required to be separated after braking thrust relieving. Therefore, the function relationship between the braking torque and braking thrust has a dead zone. This function curve can be expressed by tri-linear hysteresis model. The empirical Eq. (11) is used when modeling.

$$M_b = \begin{cases} 0 & S_t < P_0 \\ k_2(S_t - P_0) & P_0 \leqslant S_t < M_1/k_2 + P_0 \\ M_1 & M_1/k_2 + P_0 \leqslant S_t < rP \\ M_1 & rP \leqslant S_t < M_1/k_1 + P_0 \\ k_1(S_t - P_0) & M_1/k_1 + P_0 \leqslant S_t \leqslant P_{max} \end{cases} \tag{11}$$

$$k_1 = \frac{M_{sm}}{P_{max} - P_0} \tag{12}$$

$$k_2 = \frac{M_{sm}}{P_x - P_0} \tag{13}$$

where M_{sm} is the largest braking torque, M_1 the last braking torque, P_0 the pressure loss of the hysteresis, P_x the largest pressure lag, P_{max} the largest braking thrust, and rP the last braking thrust.

5.3 Model of aircraft wheels

When the aircraft is taxiing on the ground, there is friction force between the braking wheels and the ground. The product of this friction force and the rolling radius of the braking wheels is the braking torque. The rolling of the wheels is controlled by both the friction torque and the braking torque which can be expressed as follows

$$\dot{\omega} = \frac{M_j - M_b}{J_r} \tag{14}$$

$$v_r = \omega \times R_g \tag{15}$$

where ω and $\dot{\omega}$ are the angular velocity and the angular acceleration. M_j is the friction torque, M_b the braking torque, J_r the rotational inertia of one wheel, v_r the linear velocity of the wheels, and R_g the radius of the wheels.

The factors which affect the friction torque of the braking wheels include: The vertical load on the braking wheels, the rolling radius of the braking wheels, and the friction coefficient between the tires and the ground. The formula is shown as

$$M_j = f \times R_g = \mu \cdot P_m \cdot R_g \cdot n \tag{16}$$

where μ is the friction coefficient between the tires and the ground, P_m the vertical load on the main wheels, and n the number of the main tires.

6 Simulation and Analysis

In conclusion, the whole model diagram of the slip rate electric braking system is shown in Fig. 5.

It is assumed that the aircraft landing velocity is 72 m/s, and its weight is 56 000 kg. The model with the electric braking system established based on the fuzzy-PID controller with parameter self-adjustment feature is simulated in the two cases of dry runway and wet runway by MATLAB/SIMULINK.

If the control system has the PID-controller only without the fuzzy-PID controller, the simulation curves in the dry runway case are shown in Fig. 6. From the simulation results, anti-skid braking lasts 16.9 s and the distance of landing

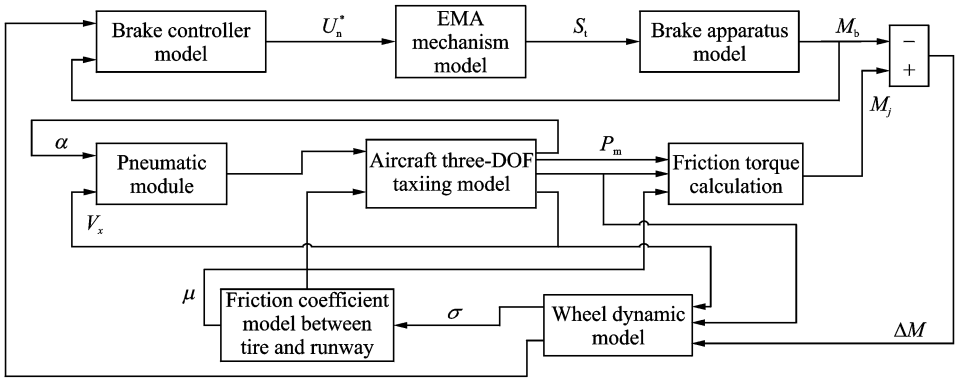

Fig. 5 Whole model diagram of slip rate electric braking system

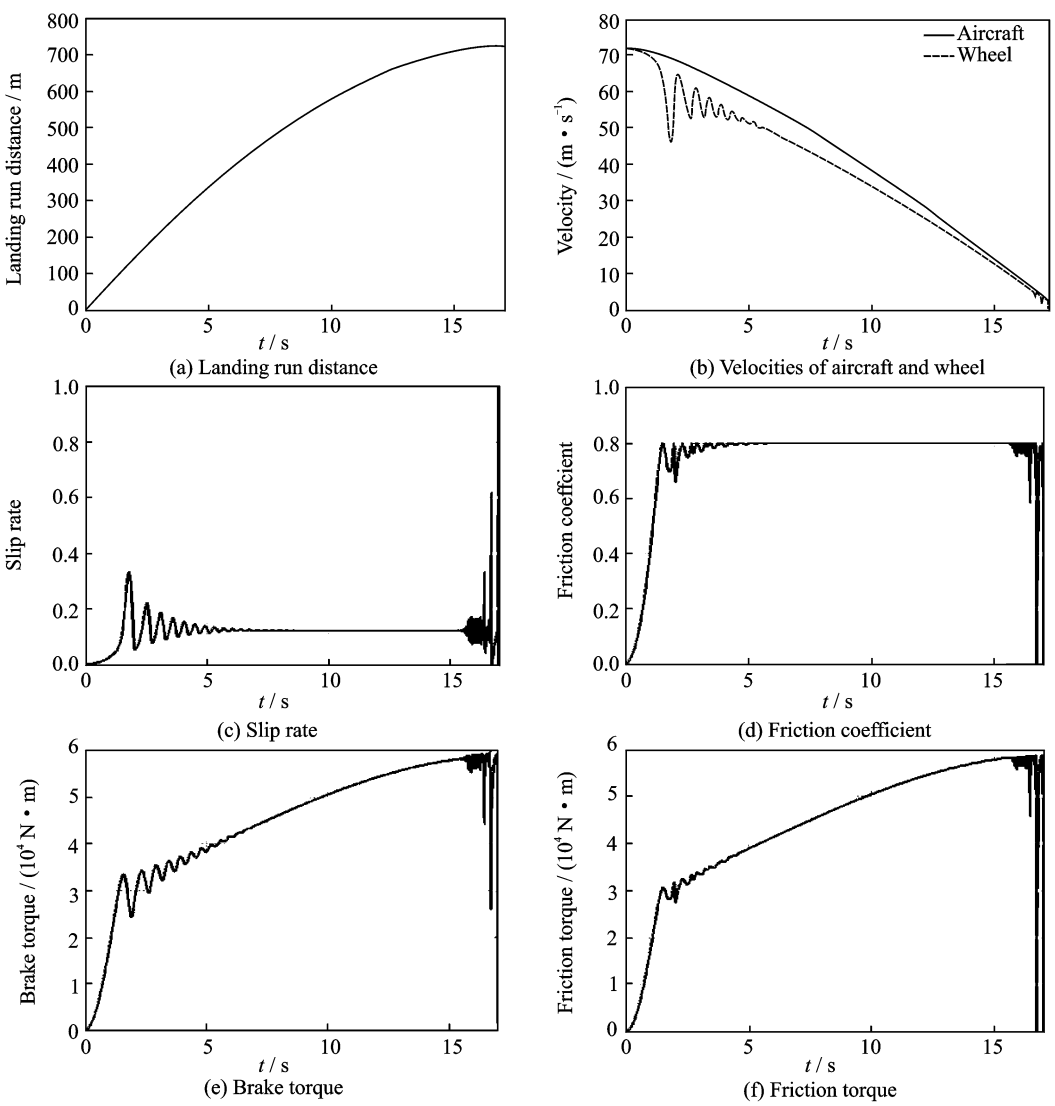

Fig. 6 Simulation curves in dry runway case with PID-controller only

run is 723 m since the brake starts when the wheel reaches the maximum velocity till the aircraft stops with the zero speed.

However, if the control system has the electric anti-skid braking system based on the fuzzy-PID controller with parameter self-adjustment feature, the simulation curves in the dry runway case are shown in Fig. 7. During the whole process, the slip rate maintains at the best with the value around 0.12 all the time. The braking efficiency is calculated as 93% according to the friction coefficient.

Compared with Fig. 6, the shock of the wheel velocity, the slip rate and the brake torque converge to a stable state faster, which indicates that with the fuzzy-PID controller, this closed-loop control system has faster response ability and better stability. Therefore, it is proved that the electric braking system established based on the fuzzy-PID control has better control effect and higher braking efficiency.

The simulation curves in the wet runway case are shown in Fig. 8. The velocity curves (Fig. 8(b)) demonstrate the slippage and skid levels of the wheel during the whole braking process. At the end of the simulation, the aircraft velocity is 8 m/s, anti-skid braking lasts 26 s and the distance of landing run is 1 198 m. Although the wheel slip appears at low velocity, the whole system still owns higher braking efficiency as approximately 82%.

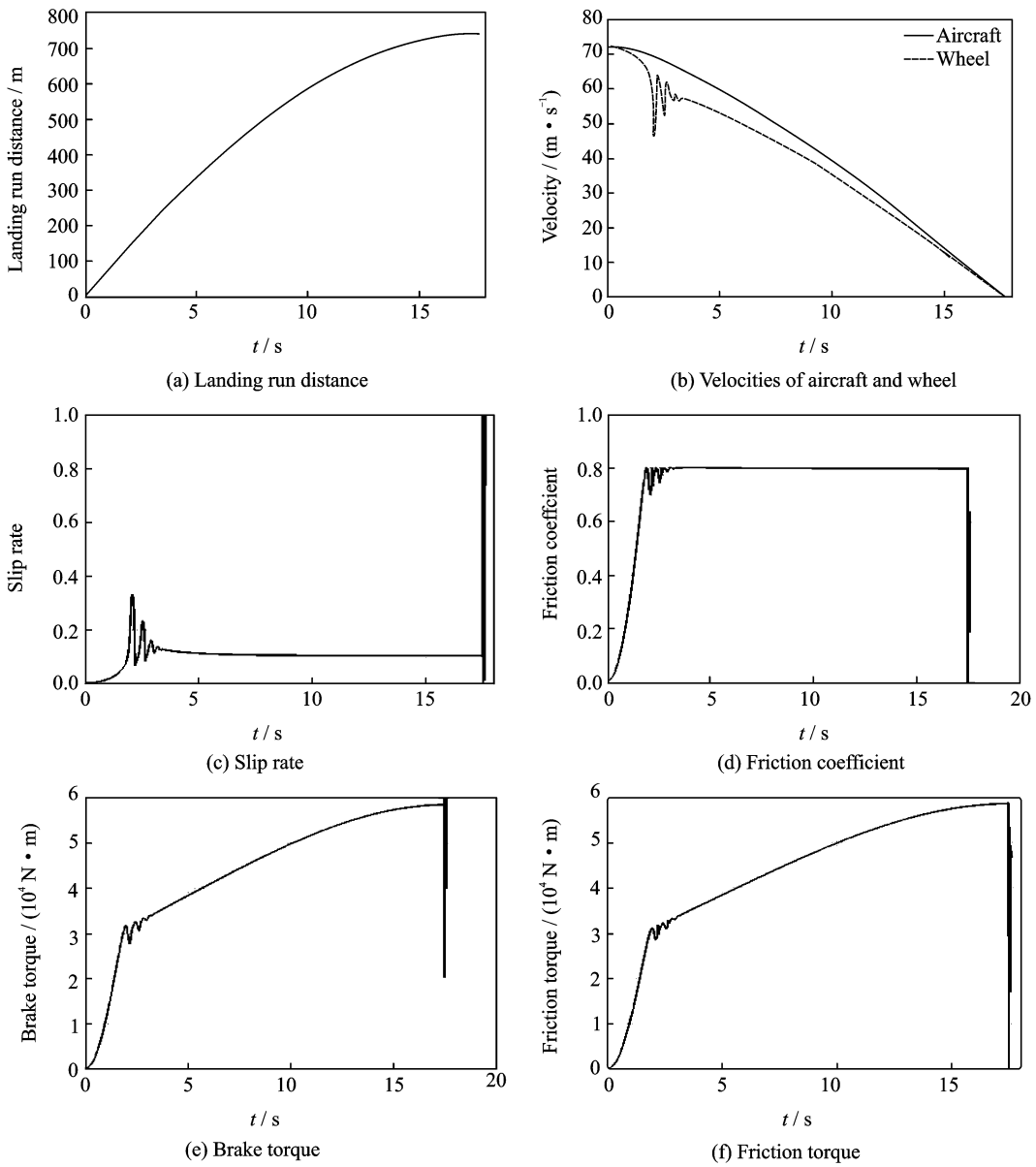

Fig. 7 Simulation curves in dry runway case with fuzzy-PID controller

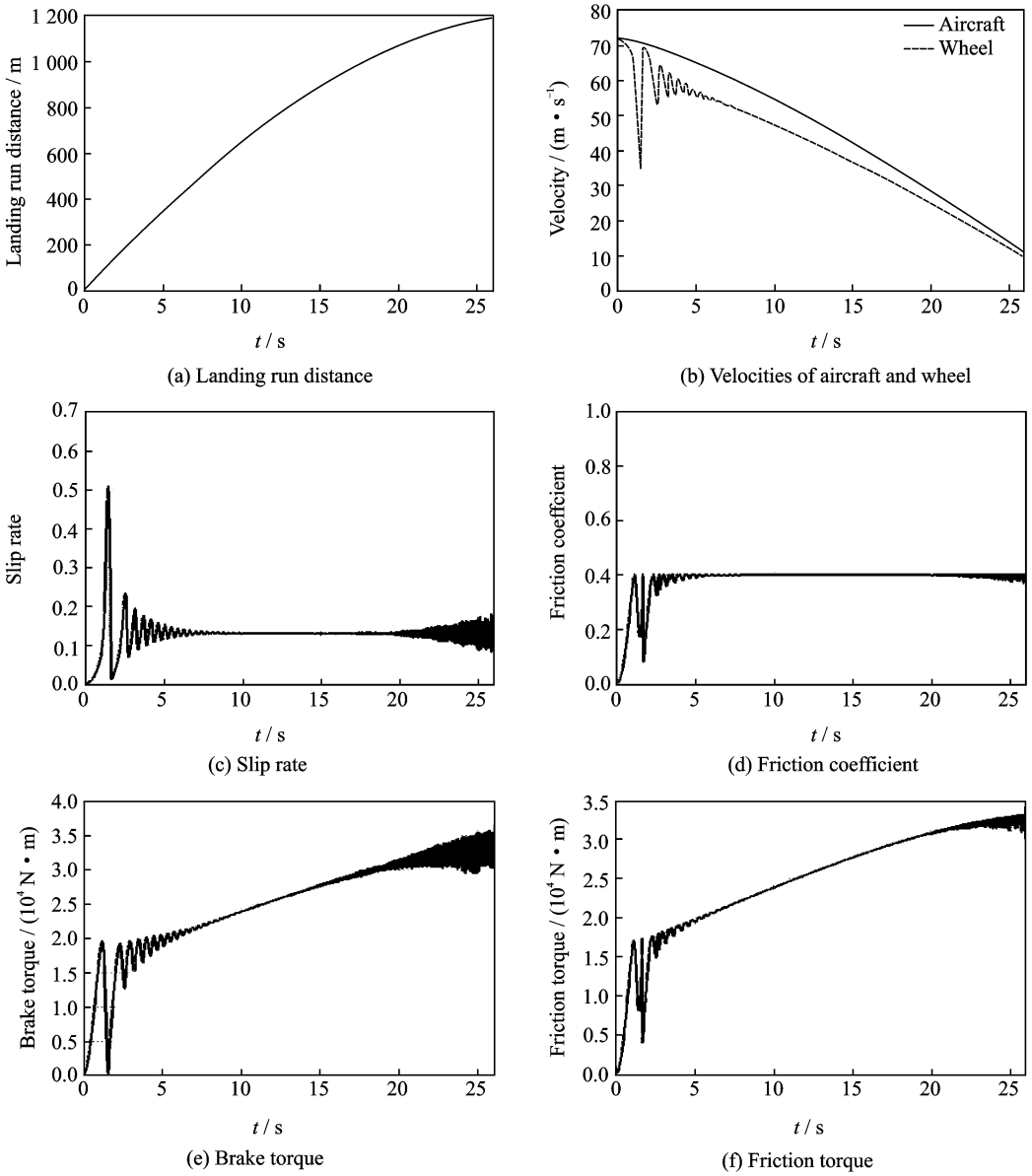

Fig. 8 Simulation curves in wet runway case with fuzzy-PID controller

7 Conclusions

(1) The working theory of the slip rate anti-skid control system and the electric braking system is analyzed to establish the slip rate control electric braking system.

(2) The electric braking system controller is designed based on the algorithms of the fuzzy-PID control with parameter self-adjustment feature to make the system reach the optimal slip rate at the shortest time and maintain constant, so that the friction coefficient will reach the largest value and the braking efficiency will be increased.

(3) The aircraft ground braking with electric braking system and fuzzy-PID controller is simulated in the two cases of dry runway and wet runway. The results show that the whole system keeps working in the state of stability and high efficiency.

References:

[1] Tang Chuanye. Simulation study of the airplane anti-skid braking system[D]. Xi'an: Northwestern Polytechnical University, 2007. (in Chinese)

[2] Tanner J A. Review of NASA anti-skid braking research[R]. SAE 821393, 1982.

[3] Stubbs S M. Tanner J A. Review of anti-skid and brake dynamics research[C]// Conference on Aircraft Safety and Operating Problems. Virginia:

NASA Langley Research Center, NASA CP-2170, 1981:555-568.

[4] Stubbs S M, Tanner J A. Behavior of aircraft antiskid braking systems on dry and wet runway surfaces: A velocity-rate-controlled, pressure-bias-modulated system[R]. NASA TN D-8332, 1976.

[5] Stubbs S M, Tanner J A, Smith E G. Behavior of aircraft antiskid braking systems on dry and wet runway surfaces: A slip-velocity-controlled, pressure-bias-modulated system[R]. NASA TP-1051, 1979.

[6] Tanner J A, Stubbs S M. Behavior of aircraft antiskid braking systems on dry and wet runway surfaces: A slip-ratio-controlled systems with ground speed reference from unbraked nose wheel [R]. NASA TN D-8455, 1977.

[7] Li Huihui. Research of the electric braking system based on the fuzzy control[D]. Xi′an: Northwestern Polytechnical University, 2003. (in Chinese)

[8] Somakumar R, Chandrasekhar J. Intelligent anti-skid brake controller using a neural network[J]. Control Engineering Practice, 1999,7:611-621.

[9] Huang You. LQ optimal simulation for aircraft antiskid brake control system[J]. Journal of Beijing University of Aeronautics and Astronautics. 2003, 29 (12): 1119-1122. (in Chinese)

[10] Wang Jisen. Nonlinear control theory and its application to aircraft anti-skid brake systems[D]. Xi′an: Northwestern Polytechnical University, 2001. (in Chinese)

[11] Xie Shihong. MATLAB R2008 dynamic simulation of control system instance tutorial [M]. Second Edition. Beijing: Chemical Industry Press, 2009. (in Chinese)

[12] Wei X H, Liu C L, Song X C, et al. Drop dynamic analysis of half-axle flexible aircraft landing gear[J]. Journal of Vibroengineering,2014,16(1):290-298.

[13] Cheng Guangren. Ball screw transmission design [M]. Beijing: China Machine Press, 1987. (in Chinese)

[14] Ruan Yi, Chen Boshi. Electric drive automatic control system—Motion control system [M]. Beijing: China Machine Press, 2009. (in Chinese)

(Executive editor: Zhang Huangqun)